Journal of Catalysis **188,** 186–202 (1999)
Article ID jcat.1999.2646, available online at http://www.idealibrary.com on IDEAL®

A Kinetic Study on the Adsorption and Reaction of Hydrogen over Silica-Supported Ruthenium and Silver–Ruthenium Catalysts during the Hydrogenation of Carbon Monoxide

David P. VanderWiel,*,[1] Marek Pruski,† and Terry S. King‡

*Iowa State University, Ames, Iowa; †Ames Laboratory, Iowa State University, Ames, Iowa; and ‡Kansas State University, Manhattan, Kansas

Received May 10, 1999; revised July 29, 1999; accepted July 30, 1999

The simultaneous adsorption and reaction of hydrogen with preadsorbed carbon monoxide was investigated over a series of silica-supported ruthenium and silver–ruthenium bimetallic catalysts to elucidate the role of site sensitivity on hydrogen adsorption and methane formation. The specific rate of methane synthesis, which is a direct measure of the catalyst activity toward the Fischer–Tropsch synthesis, measured at 460 Torr and temperatures from 400 to 500 K, varied from 0.01×10^{-3} to 3×10^{-3} s^{-1}. As little as 3% Ag reduced the methanation rate of Ru by 80%. The temperature dependence of the turnover frequency showed that the apparent activation energy for methanation dropped from 24 kcal mol^{-1} for the monometallic ruthenium case to 18 kcal mol^{-1} for the bimetallic case. Since silver does not adsorb or react with either hydrogen or carbon monoxide, these results show that silver does not act merely as a dilutant in the bimetallic system. These observations are elucidated in terms of a new model for surface-sensitive hydrogen adsorption, termed "portal site mediated adsorption," where low-coordination edge and corner sites on the catalyst surface act as sinks for rapid, dissociative adsorption of weakly bound, highly mobile surface hydrogen. *In situ* **^{1}H-NMR measurements of surface hydrogen coverages during reaction were used to confirm the kinetic model treatment of the reaction data.** © 1999 Academic Press

Key Words: **Fischer–Tropsch; ruthenium; silver; bimetallic catalysts; hydrogen adsorption; carbon monoxide hydrogenation.**

INTRODUCTION

Since Sabatier and Senderens (1) first produced methane by reacting hydrogen and carbon monoxide over a nickel catalyst in 1902, the catalytic hydrogenation of carbon monoxide over the Group VIII transition metals has been an area of increasing focused research for nearly a century. Fischer and Tropsch (2) reported on the synthesis of higher hydrocarbons using iron and cobalt catalysts in 1923, and today the term Fischer–Tropsch synthesis is reserved for processes which produce C_2 and higher hydrocarbons (usually linear alkanes and alkenes) and/or oxygenates (usually *n*-alcohols), as opposed to methanation processes, where methane is the primary product. While the two processes often occur separately in industry and are sometimes treated separately in the literature, they are intimately linked. This owes to the fact that, in the absence of heat and mass transfer limitations, both processes involve the same rate-determining surface reaction and depend strongly on interactions between similar catalyst surfaces, reactants, and adsorbed intermediates.

Fischer–Tropsch synthesis (FTS) is the only existing major alternative to petroleum and natural gas as a source for liquid hydrocarbon petrochemicals. Because the volumetric energy content of such liquids is significantly greater than gaseous hydrocarbons, and because their combustion produces less pollution than solid fuels, their importance in industry cannot be overstated (3). At present, industrial FTS processes are the third largest consumers of syngas (4). As coal gasification technologies and steam-reforming processes for natural gas become more advanced, the use of syngas as a source of carbon monoxide and hydrogen for FTS is becoming increasingly economically feasible. Currently, it is estimated that coal and natural gas reserves outweigh those of crude oil by 9 : 1 (5).

Although the catalytic hydrogenation of carbon monoxide has been a subject of considerable investigation for many years, its increasing economical attractiveness as an industrial source of hydrocarbons has recently led to a search for more active and selective catalysts. A fundamental problem in the development of such catalysts in an incomplete knowledge of the operative surface processes, due in large part to the inability to accurately measure surface concentrations of reactant species during reaction. Specifically, the concentration of surface hydrogen proves difficult to estimate using normally revealing techniques, such as transient isotopic exchange, due to kinetic isotope effects. Knowledge of such concentrations is essential to the determination of the mechanisms of adsorption and

[1] To whom correspondence should be addressed: Pacific Northwest National Laboratory, P.O. Box 999, MSIN K8-93, Richland, WA 99352. Fax: (509) 376-5106. E-mail: david.vanderwiel@pnl.gov.

0021-9517/99 $30.00
Copyright © 1999 by Academic Press
All rights of reproduction in any form reserved.

reaction since many kinetic parameters are concentration dependent.

Several authors have written excellent reviews in recent years of the catalytic hydrogenation of CO. Recently, *Topics in Catalysis* dedicated an entire issue (7) to industrial hydrocarbon production, and Adesina (8) reviewed catalyst design, reaction kinetics and mechanisms, and industrial reactor development. In addition, there have been recent general reviews on the Fischer–Tropsch synthesis by Dry (5) and Bartholomew (9) and on reactions of syngas by Wender (4). More relevant to the present study, Somorjai (10) reviewed the catalytic synthesis of methane and methanol via CO hydrogenation.

In general, the Group VIII transition metals and their oxides are good hydrogenation catalysts, and the modern work of Vannice (11) shows that the metals used by early researchers as catalysts were good choices. While iron and cobalt are the metals of choice for commercial FTS processes, the exceptional properties of ruthenium has made it the subject of substantial investigation, especially in recent years (6, 12–14). As the most active Group VIII transition metal, ruthenium is active at temperatures as low as 373 K, produces the largest hydrocarbons, does not form oxide phases with catalyst supports (15), and provides researchers with simple product distributions. In addition, under most conditions, inactive carbide formation does not occur on the metal surface. Perhaps most importantly, carbon monoxide dissociates easily and at lower temperatures than other active Group VIII metals, resulting in very low oxygenate formation compared to Os, Rh, Ir, Pd, and Pt, on which carbon monoxide does not usually dissociatively adsorb (10, 16).

An interesting result of kinetic analysis of the FTS mechanism is that often the same governing equation results from different mechanistic derivations. Both the power rate law and Langmuir–Hinshelwood (LH) forms of rate equations are generally agreed to accurately describe the kinetics on FTS and methanation catalysts. However, these equations reflect an underlying problem in the development of kinetic expressions, where macroscopic parameters such as partial pressures are used to describe microscopic processes such as adsorption, dissociation, and surface diffusion. This problem is primarily due to the fact that many microscopic parameters, such as surface species coverages on the catalyst, are difficult to measure during reaction. Therefore, researchers are forced to either estimate such parameters or relate the rate to macroscopic parameters. Such is the case for steady-state isotopic transient kinetic analysis (SSITKA) studies, where kinetic isotope effects do not allow accurate calculation of hydrogen coverages during reaction.

The mechanism of carbon monoxide hydrogenation consists of five primary steps: reactant adsorption, chain initiation, chain growth, chain termination, and product desorption. Methane can form at any time during the course of chain propagation if hydrogen is present in sufficient surface concentrations to completely hydrogenate a surface carbon species. While methane is the thermodynamically favored product under all conditions, the ability to suppress this reaction in favor of chain growth is the hallmark of a good Fischer–Tropsch catalyst. In the absence of gas phase CO, as in CO preadsorption techniques, methane is formed almost exclusively (3).

For the present discussion, an approach similar to that of Alstrup (17) for methanation over nickel is used to develop a "microkinetic" model of the hydrogenation of carbon monoxide to methane. First, the following assumptions are made: at low conversions, reactions involving CO_2 are not important; the sticking probabilities for H_2 and CO reveal that their rates of adsorption are usually rapid compared to the rate of methane formation (18); the formation and desorption of H_2O from adsorbed oxygen is also rapid, and so CO dissociation is assumed to be irreversible; under conditions of low conversion and small methane partial pressures, the formation and desorption of methane is also assumed to be rapid and irreversible. This leads to the following simplified reaction sequence:

$$\begin{aligned} 2M + H_2 &\leftrightarrow 2M\text{–H}, \\ M + CO &\rightarrow M\text{–CO}, \\ M\text{–CO} + M\text{–H} &\rightarrow M\text{–CH} + M\text{–O}, \\ M\text{–O} + 2M\text{–H} &\rightarrow H_2O + 3M, \\ M\text{–CH} + M\text{–H} &\rightarrow M\text{–CH}_2 \rightarrow\rightarrow CH_4, \end{aligned}$$

in which the series of reactions leading to methane are assumed to occur at the same rate under the steady-state approximation. Using the common assumption that the rate-limiting step is the hydrogenation of surface carbon species,

$$M\text{–CO} + M\text{–H} \rightarrow M\text{–CH} + M\text{–O},$$

the rate of reaction may then be written as

$$\text{rate} = k\theta_H\theta_{CO}. \qquad [1]$$

This result is quite similar to a simplified reaction sequence for methanation, reflective of the overall kinetics of the reaction, derived by Biloen and Sachtler (3). Bajusz and Goodwin (19) also presents a similar mechanism for methanation over Ru/SiO_2.

As mentioned earlier, the key to many of the differences seen in catalyst activities and product distributions during FTS is believed to stem from the adsorption and dissociation behavior of carbon monoxide on the surface. Metals on which CO is typically dissociatively adsorbed include Fe, Ru, and Co (20–22), while CO is molecularly adsorbed on Os, Ir, Pd, and Pt (10, 16). Catalytic activity is higher on surfaces where CO dissociates; thus, it should not be surprising

that CO adsorption on ruthenium is quite strong and occurs molecularly only at temperatures near and below 300 K (4). For adsorption on ruthenium at room temperature, it is likely that linear species are predominant, with a 1 : 1 Ru-to-CO ratio in the absence of gas phase CO. Gupta *et al.* (23) also reported a 1 : 1 ratio on Ru/TiO_2 catalysts.

The adsorption of hydrogen on ruthenium at low pressures has been a subject of considerable research (24), while several higher pressure studies have been conducted in our laboratories (25–28). The dissociative adsorption of hydrogen usually occurs in a 1 : 1 metal-to-hydrogen ratio, although ^{1}H-NMR results have revealed that coverages far in excess of this value are common on ruthenium catalysts at higher pressures (25). Two types of chemisorbed hydrogen have been identified by FTIR (29) and ^{1}H-NMR (30) and are referred to as weakly (or reversibly) and strongly (or irreversibly) bound hydrogen. The weakly bound hydrogen is known to exchange rapidly with the gas phase and the support (25) and to be highly mobile (31). There is believed to be a stronger interaction between adsorbed hydrogen and low-coordination edge and corner "defect-like" sites on ruthenium particles, and the weakly bound hydrogen was found to be at least partially associated with these sites (30).

Recently, Gupta *et al.* (23, 32–33) studied the coadsorption of CO and H_2 on polycrystalline Ru and Ru/TiO_2 and found that these processes occur at distinct Ru sites in a 1 : 1 ratio. The interaction of adsorbed CO and H on ruthenium is facilitated by empty, low-lying *d* valence orbitals, a condition that also favors CO dissociation. For these reasons, the high activity of Ru toward FTS should not be surprising.

It is important to mention that adsorption processes have been shown to be structure sensitive. Since adsorption and dissociation on a surface atom are strongly dependent on the electronic environment of the atom, and this environment is strongly affected by neighboring atoms, it is not surprising that sites with different coordinations exhibit different adsorption characteristics. For example, Bernasek and Somerjai (34) have reported that hydrogen adsorption and dissociation occur more efficiently at low-coordination sites on platinum. In addition, Marcelin *et al.* (35) used frequency response chemisorption techniques to identify "kinetically distinct" adsorption sites for hydrogen on supported rhodium.

In general, CO hydrogenation is considered to be structure insensitive (9, 36). For this reason, it is assumed that each surface atom in this study represents an active surface site, or at least that the total number of surface atoms and active sites are directly proportional (36). The structure insensitivity of nickel surfaces for CO hydrogenation is well documented (11, 18, 20, 37) for a variety of both supported catalysts and single crystals. There has been less agreement among researchers studying other Group VIII metals, with evidence for crystallite size, metal loading (and thus dispersion), and support effects (9, 38). More recently, however, several studies on Fe, Co, Ni, Mo, Ru, and Rh (38, 39–42) have shown that pure, well-reduced catalysts can yield rates which are independent of dispersion and surface structure. For example, Kelley and Goodman (39) found very similar rates and activation energies for methanation over the Ru(110) single crystal and the Ru(001) basal plane, which have quite dissimilar structures. Therefore, if it assumed that findings which suggest CO hydrogenation to be structure insensitive are extended to include ruthenium catalysts such as those in this study, the only further consideration required to allow for comparison of specific rates is accurate determination of the metal dispersion of these catalysts.

An important and interesting phenomenon in heterogeneous catalysis is the synergistic effect often observed upon addition of Group IB metals (Cu, Ag, and Au) to transition metal catalysts. While the added metal may not interact directly with the adsorbed species during reaction, their catalytic effect is often more than the sum of the individual contributions of the two metals. Thus, the Group IB metal apparently affects the activity of the transition metal without necessarily directly taking place in the reaction itself. A considerable amount of research has been conducted on Cu–Ru catalysts (43–46), but less is known about Ag–Ru (26, 47–52) and Au–Ru (31) catalysts.

The Ag–Ru bimetallic system is of particular interest in CO hydrogenation studies due to the fact that silver does not appreciably adsorb either hydrogen or carbon monoxide (53) and thus does not take part in surface reactions. In addition, hydrogen adsorbed on Ru does not spill over to Ag. It is also advantageous to utilize the fact that Ag atoms preferentially occupy certain locations in bimetallic ruthenium particles. Our earlier Monte Carlo simulations of Group IB–Ru systems (49, 52) reveal that Cu, Ag, and Au atoms migrate to the surface of bimetallic particles, tend to cluster with like atoms, and preferentially occupy low-coordination edge, corner, and other "defect-like" sites. Figure 1 (52) shows the results of several simulations which demonstrate this behavior. In contrast to systems like Pt–Rh (top row), which exhibit random mixing of platinum atoms (light spheres) with rhodium atoms (dark spheres) at all loadings, bimetallic systems such as Cu–Ru (bottom row) exhibit strong segregation of copper atoms (dark spheres) from ruthenium atoms (light spheres). The Group IB atoms segregate in three ways: they tend to migrate out of the bulk to locations on the catalyst surface, they tend to group together with other IB atoms, and they preferentially occupy low-coordination edge and corner sites. In Ag–Ru bimetallic systems, nearly complete occupation of these sites occurs at Ag contents below 20 at.% (total metal) (49). Ensemble effects in Ag–Ru catalysts are also not believed to be operative, as Ag does not break up ensembles in Ru (50, 52, 54). Electronic effects, which may affect the vacant *d* orbitals in Ru, are also not believed to be present (27, 51). Therefore, other mechanisms which explain the behavior of Ag–Ru catalysts must be investigated.

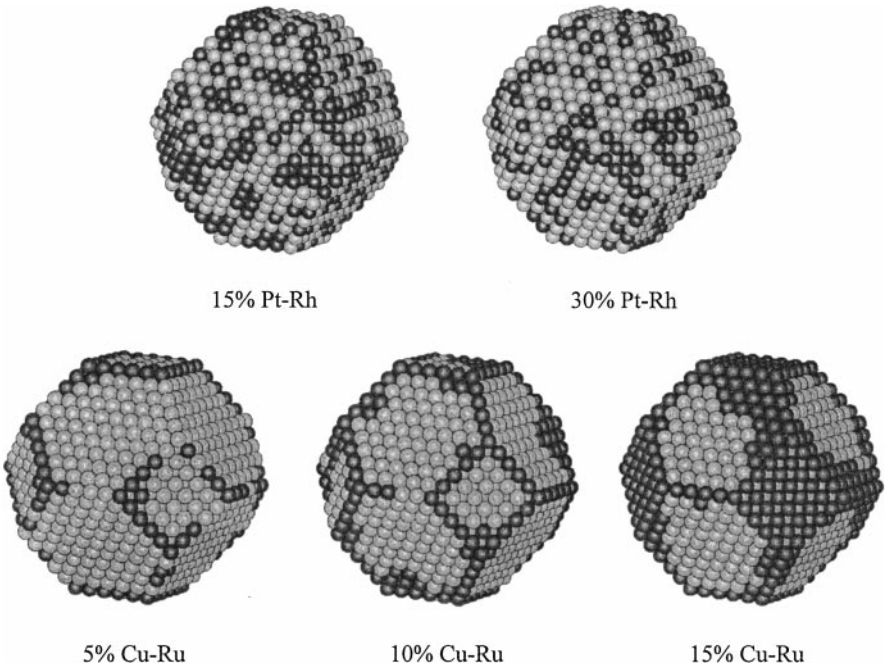

FIG. 1. Monte Carlo atomistic simulation of bimetallic particles (52).

METHODS

For this study, carbon monoxide is preadsorbed onto the catalyst surface prior to reaction. Using this technique, a surface initially saturated with CO is achieved and, upon exposure to hydrogen gas at reaction temperatures, the initial rate of methane formation is a measure of the surface activity. The generalized chemical equation for this process may be represented as

$$M\text{–CO} + 3\text{H}_2 \rightarrow \text{CH}_4 + \text{H}_2\text{O}.$$

The rate measured this way is done without the exact knowledge of which step in the reaction mechanism it represents. This is important to the analysis of data when it is possible that the rate-limiting process may be changing upon addition of Ag to the Ru catalyst, as will be discussed later. Biloen and Sachtler (3) reviewed hydrogenation of preadsorbed CO in detail, and Bajusz and Goodwin (19) recently studied methanation over Ru/SiO_2, noting that such studies are directly relevant to hydrogenation reactions because the rate-limiting steps, usually hydrogenation of surface carbon species, are the same. Also, similar temperature-programmed surface reaction (TPSR) methanation studies, where preadsorbed CO is reacted with hydrogen, have been conducted by many researchers, and the results have been found to correlate well with steady-state experiments (55).

Silica-supported ruthenium catalysts containing 4 wt% ruthenium metal were prepared from solutions of 1.5 wt% ruthenium nitrosyl nitrate. The incipient wetness preparation technique was used by impregnating silica (BET surface area, 300 $m^2\ g^{-1}$) with the ruthenium solution to form a slurry, which was allowed to dry at room temperature overnight and then at 383 K for 2 h. The Ru–Ag bimetallic catalysts containing Ag : Ru = 3 : 97, 10 : 90, 20 : 80, and 30 : 70 (corresponding to 0.133, 0.480, 1.08, and 1.85 wt% Ag, respectively) were prepared by coimpregnation of silver nitrate with the ruthenium solution. The ruthenium loading in the bimetallics remained at 4 wt%. The catalyst samples were washed with hot deionized water after reduction to remove sodium and chlorine contamination. In most cases, the same catalyst samples that were used in previous microcalorimetry studies were used in this study. For the ^{1}H-NMR experiments, a catalyst sample prepared for an earlier study (56) was used. All catalyst dispersions were measured by hydrogen chemisorption using a custom-built adsorption apparatus described previously (30). An optimized volumetric technique from Uner *et al.* (27) was used for the chemisorption experiments. Dispersion values for the catalyst samples used in this study are presented in Table 1.

TABLE 1

Catalyst Sample Dispersions

Catalyst[a]	Volumetric dispersion
4% Ru/SiO_2	0.261
4% Ru/SiO_2 (NMR)	0.20[b]
3% Ag–Ru/SiO_2	0.258
10% Ag–Ru/SiO_2	0.121
20% Ag–Ru/SiO_2	0.180

[a] All catalysts contain 4 wt% ruthenium; silver content shown is the at.% of total metal.

[b] Determined via ^{1}H-NMR.

A custom-built glass and stainless steel reaction and adsorption manifold (57) was constructed to conduct the kinetic studies. The manifold was supplied with research-grade hydrogen and carbon monoxide and zero-grade helium through a multiport stream selection valve. A turbomolecular pump, backed by a mechanical pump, was used for evacuation. A Pyrex reaction cell, connected to the manifold via vacuum fittings, was placed inside a custom-built furnace connected to a temperature controller. The sample cell was connected to a high-vacuum stainless steel manifold via needle valve and fused-silica capillary. The manifold contained a quadrupole mass spectrometer probe. A turbomolecular pumping station allowed evacuation of the manifold to about 2×10^{-6} Torr (1 Torr = 133.3 N m^{-2}), as measured by thermocouple and cold cathode gauges. An A/D interface was used to connect the spectrometer to a personal computer for control and data acquisition.

The nuclear magnetic resonance (NMR) experiments utilized a custom-built spectrometer operating at a proton resonance frequency of 250 MHz. This apparatus is the same as that described elsewhere (25), except for the addition of a digital PC interface to control pulse programming and a rapid data acquisition system. A custom Pyrex *in situ* probe containing a catalyst sample was used for dynamic measurements of hydrogen surface coverages on the catalyst surface during reaction with preadsorbed carbon monoxide.

Prior to the NMR experiments, catalyst samples were loaded into a Pyrex reaction cell and reduced *in situ* by exposing the catalyst to 1 atm of hydrogen in successive 30-min doses for a total of 2–3 h at 673 K. The sample was evacuated for 2–3 h at 673 K and then overnight at room temperature. This procedure was conducted between each experimental reaction run. Prior to reaction, the catalyst was exposed to 1 atm of CO at room temperature for 1 h. The cell was then evacuated for 30 min to remove weakly bound CO, heated to reaction temperatures (between 400 and 525 K), and exposed to 460 Torr of hydrogen while monitoring the reaction with the spectrometer or monitoring hydrogen adsorption with the NMR. Under these conditions, with essentially no gas phase CO present, the only carbon reaction product is CH_4. While the hydrogen pressure was maintained at 460 Torr, data was gathered for about 20 min, until the initial responses leveled for CH_4 and H_2O in the gas phase and H adsorbed on Ru. The sample was then heated to 673 K to drive the surface reaction to completion so that the total amount of carbon species initially present on the catalyst could be calibrated to the spectrometer signals. After reaction, the sample was reduced in hydrogen, according to the procedure outlined above, to prepare it for the next experiment. The order of metal loadings for the Ag–Ru bimetallics as well as the temperatures used for each run were randomized to eliminate any effects of catalyst deactivation or hysteresis in the data. In addition, each metal loading and temperature combination was reproduced at least once.

Under the experimental conditions used in this study, the CO conversion was low during the maximum rate portion of the experiment (typically less than 5%). Mass and heat transfer limitations were found to be present only at higher temperatures, and when these limitations were evident, the data was not used in further kinetic analysis. Catalyst deactivation was monitored by tracking total methane formation through a calibration factor for each experiment with a given catalyst sample. Specific rates are reported as maximum turnover frequencies, TOF (also known as turnover rate, TOR) in units of moles of CH_4 formed per mole of active site (surface Ru atom) per second. Finally, the widest possible temperature range was utilized, and the experimental design was randomized.

The ^{1}H-NMR spectra peaks corresponding to adsorbed hydrogen and silica support hydroxyl groups were deconvoluted by computer, assuming symmetry around the hydroxyl peaks. After deconvolution of these peaks, the areas under the hydrogen-on-ruthenium peaks were calculated to correlate with the hydrogen uptake by the catalyst. Their relative intensities were calculated by assuming that the hydroxyl group peak height remained constant on the time scale of the experiments. This approximation has been verified via separate measurements.

RESULTS

The turnover frequencies, measured at temperatures from 400 to 474 K, are plotted in Fig. 2. The TOF varies from around 0.0001 to 0.01 s^{-1} over this temperature range. As can be seen, a nearly linear trend is apparent for a lower temperature range, with negative deviations from this trend above 450 K. The reasons for this deviation are discussed later. Accordingly, only the data for the three lowest temperatures were used in the kinetic analysis of the Ru/SiO_2 catalyst. Figure 3 shows the Arrhenius plot along with the results of a linear regression of the lower temperature data. The slope of this line yields an apparent activation energy of 23.2 kcal mol^{-1}, with the linear regression yielding a standard error of $\pm$1.7 kcal mol^{-1}.

Next, the results from these studies were correlated with those for an identical ^{1}H-NMR study conducted at 400 K, the same temperature at which previous H_2 microcalorimetry studies were conducted (51). During the course of the reaction, two H/Ru resonances, corresponding to weakly adsorbed hydrogen, were monitored as the reaction progressed. Figure 4 shows the development of these resonance peaks, at approximately -45 and -55 ppm, upon exposure of the CO-saturated catalyst to 460 Torr of H_2. The resonance peak at $\sim$0 ppm is due to hydroxyl groups on the silica support. Figure 5 shows the resulting value for the ratio

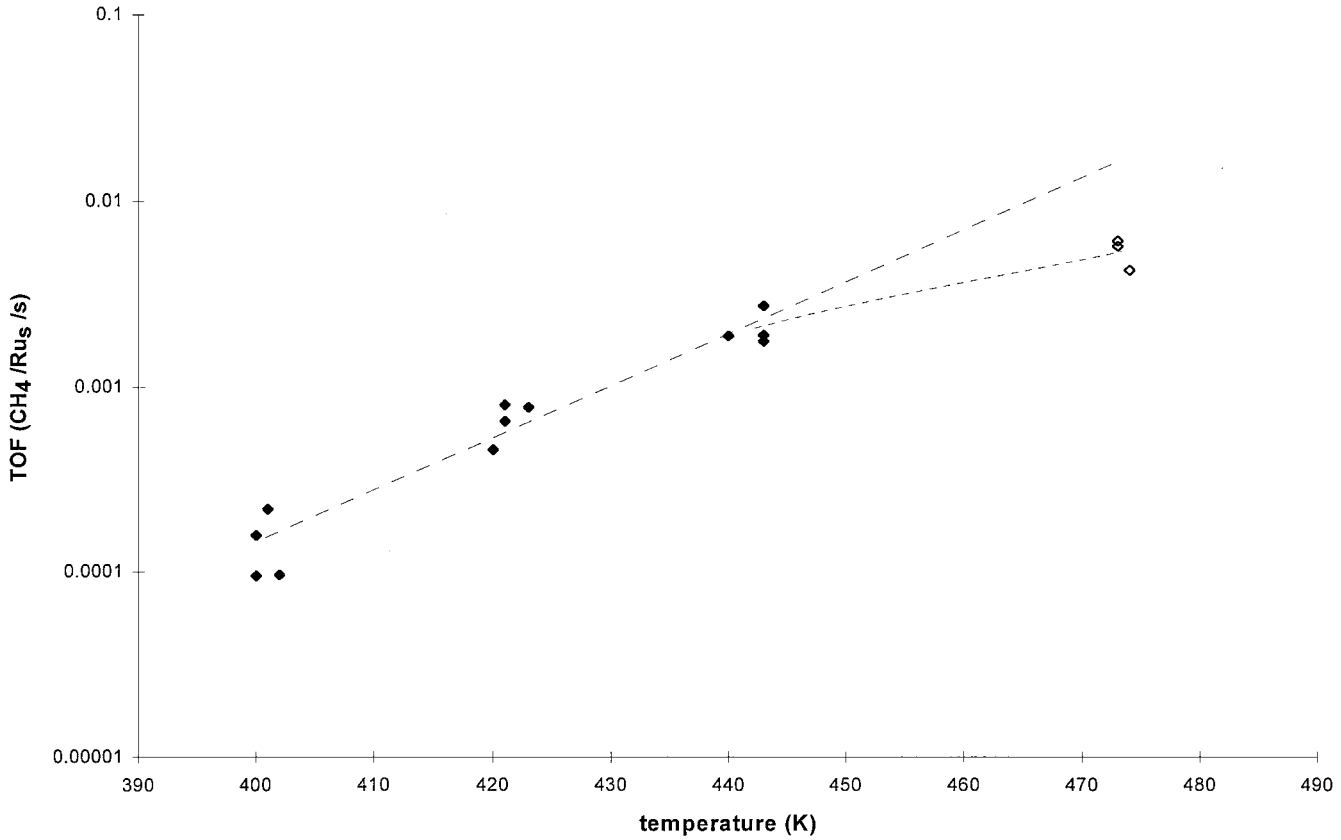

FIG. 2. Turnover frequencies for methane formation over 4% Ru/SiO_2.

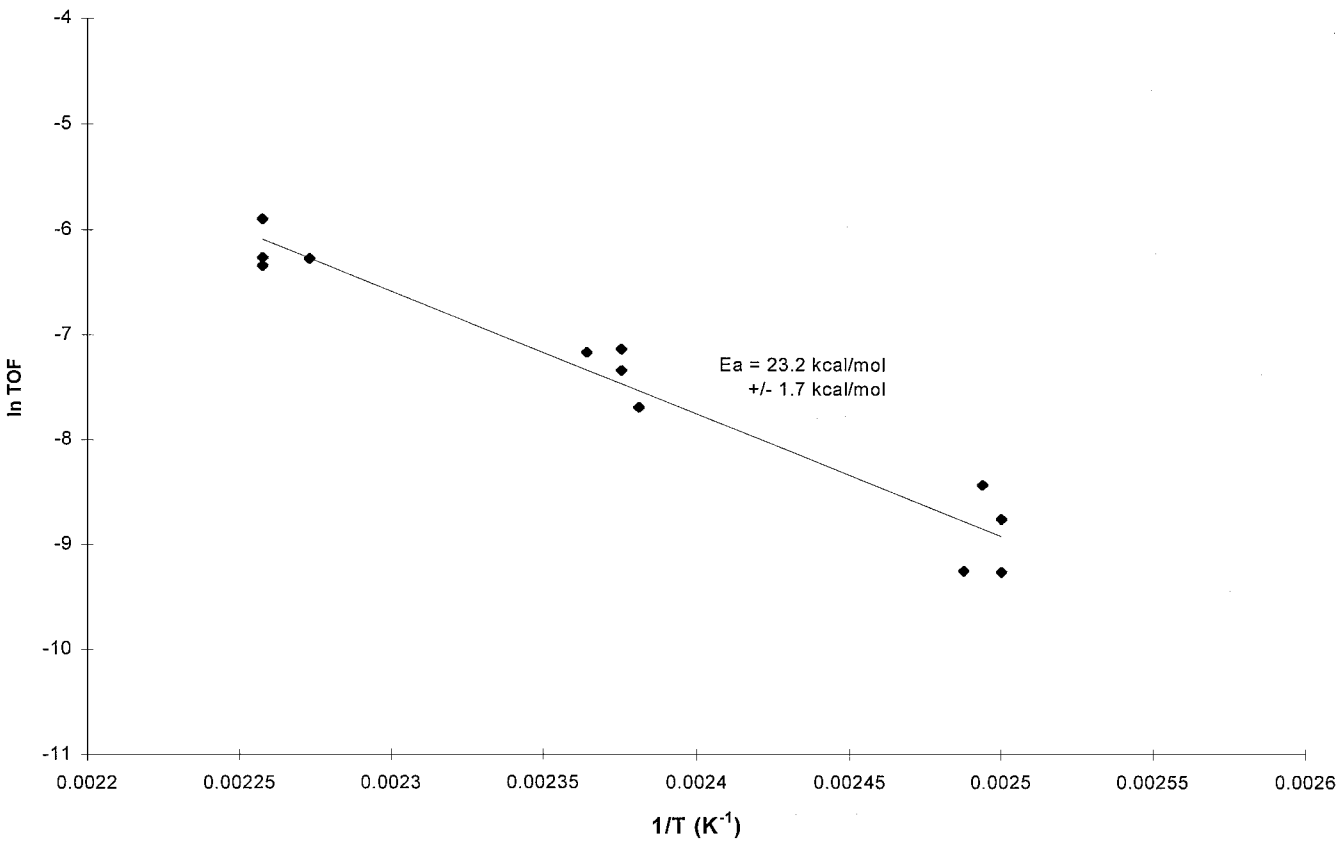

FIG. 3. Arrhenius plot for methane formation over 4% Ru/SiO_2.

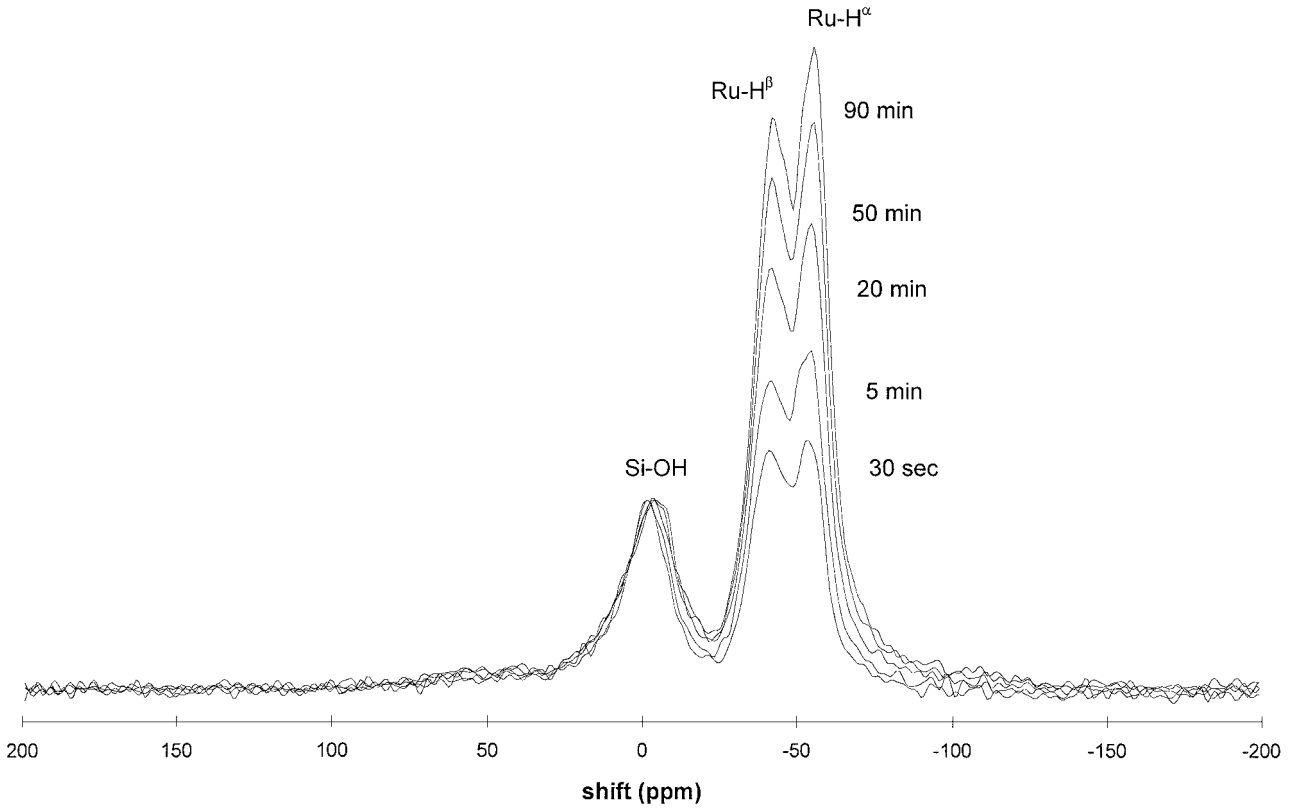

FIG. 4. Hydrogen adsorption on 4% Ru/SiO_2 during CO hydrogenation (400 K, 460 Torr).

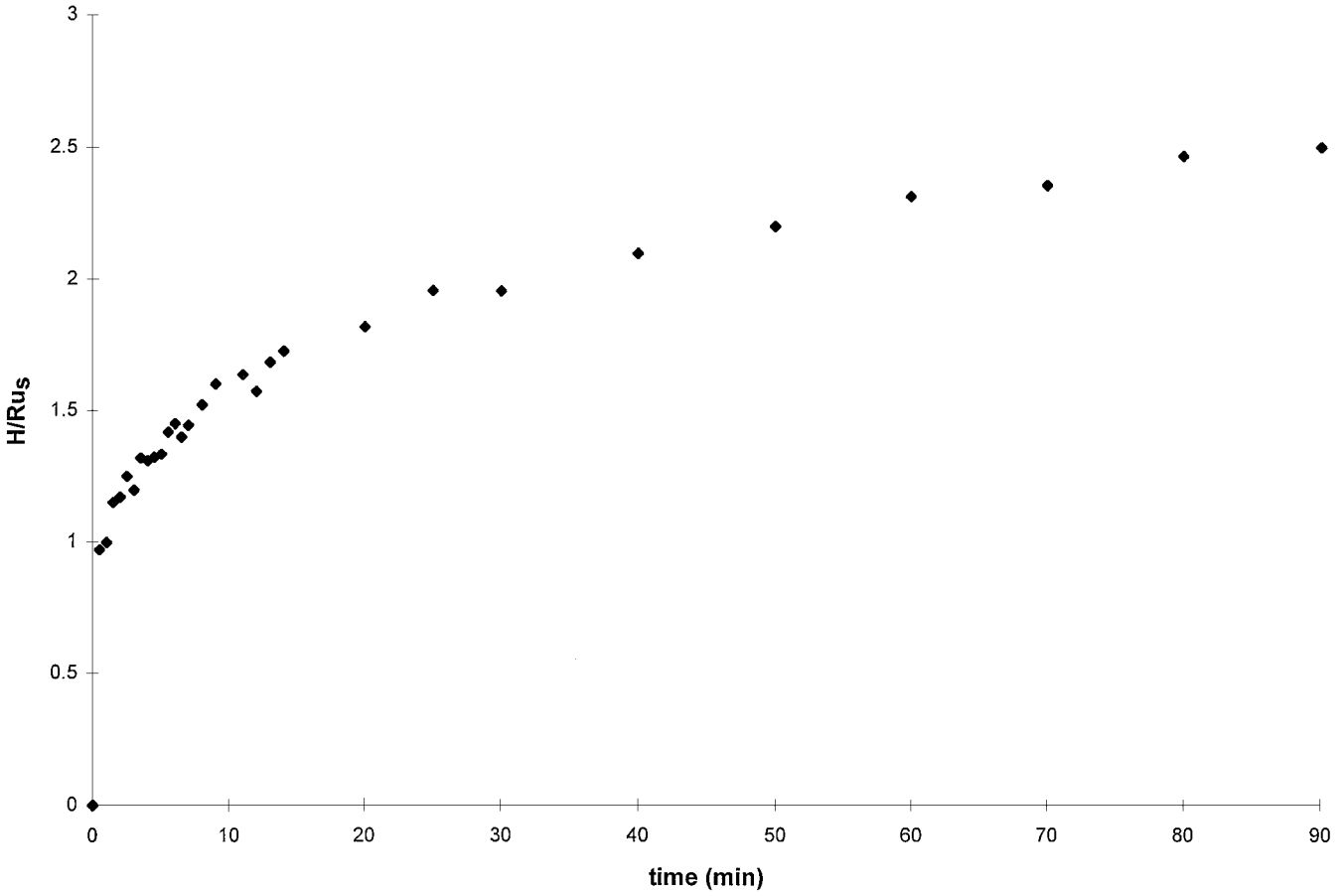

FIG. 5. Hydrogen coverage during methanation over Ru/SiO_2 (400 K, 460 Torr).

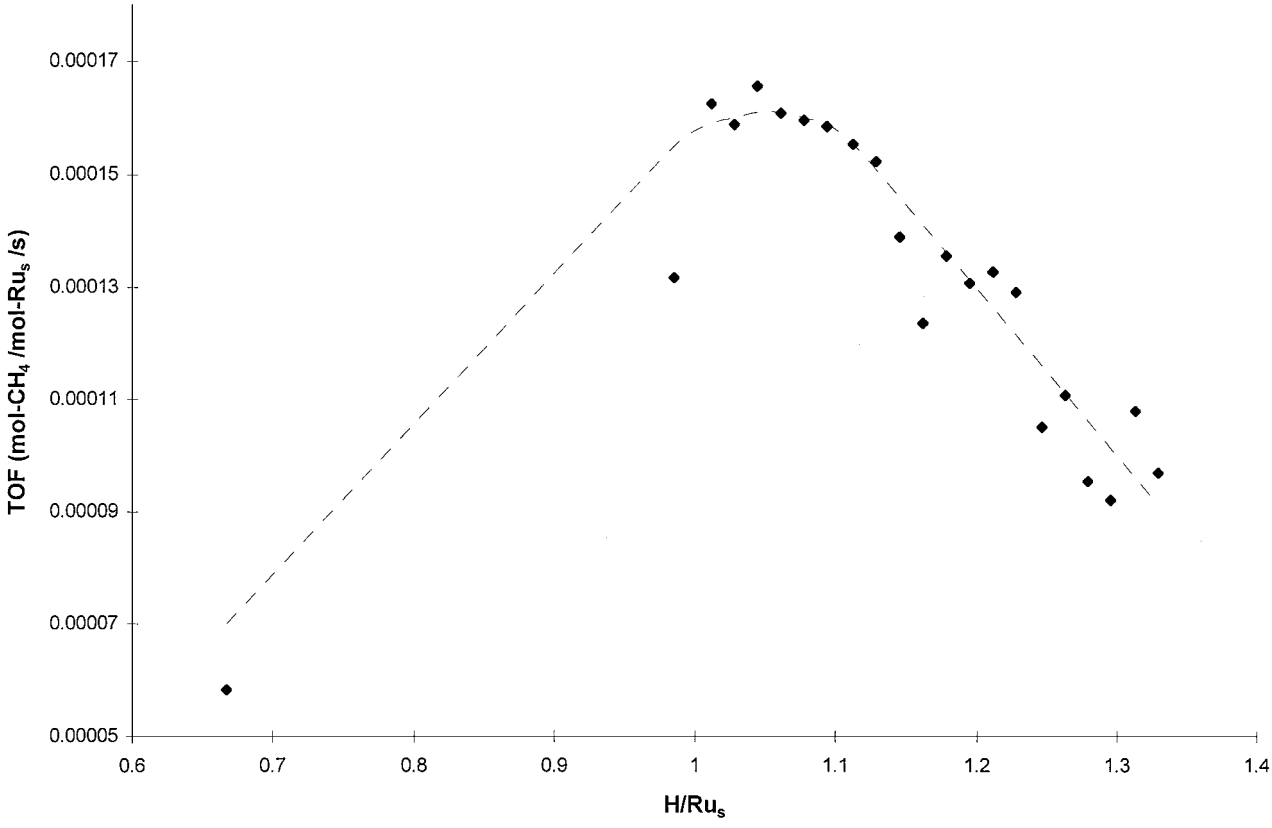

FIG. 6. Change in methanation rate with hydrogen coverage over Ru/SiO_2 (400 K, 460 Torr).

H/Ru_s (adsorbed hydrogen per surface ruthenium atom) as a function of time during reaction at 400 K. As can be seen from this figure, upon exposure of the CO-saturated catalyst to 460 Torr of hydrogen gas, the H/Ru_s signal rises rapidly at first to a value of about 1, after which adsorption occurs more slowly. After an exposure time of 90 min, the coverage approaches an asymptotic value of about 2.5 H/Ru_s. Figure 6 shows the correlation between the reaction rate and hydrogen adsorption, where the time dimension has been removed to correlate the rate of methane formation as a function of hydrogen coverage. As this figure shows, the rate increases rapidly to a value of about 1 H/Ru_s, and then remains relatively constant until a value of approximately 1.1 is reached, after which the rate of methane formation decreases rapidly. Note that, for clarity, some of the lower coverage data, which give rise to the regression line, is not included. After surface CO is depleted, hydrogen continues to adsorb slowly onto the metal surface.

Similar experiments were repeated for a series of Ag–Ru/SiO_2 bimetallic catalysts with silver contents of 3, 10, 20, and 30 at.% (of total metal content). As little as 3% Ag causes the formation of methane to slow significantly, with additional Ag having a less pronounced effect. In addition, as discussed below, the temperature dependence of this rate was also shown to decrease. The decrease in the rate of methane formation is present at all temperatures studied, as shown in Fig. 7, where the monometallic data are included for comparison. The TOFs for the 3 and 10% Ag catalysts showed little difference from one another, but were both about 80% lower than those in the monometallic case. Further addition of 20–30% Ag resulted in rates that were about 95% lower than those of the monometallic catalyst.

Figure 8 shows the effect of Ag addition on the apparent activation energy for methane formation. From this figure, it is apparent that the net effect is to lower the activation energy from its initial value of about 23 kcal mol^{-1} to about 18 kcal mol^{-1}. The activation energies for 3, 10, 20, and 30% Ag are all approximately constant within experimental error. The error bars in this figure represent the standard deviation in the activation energy obtained from a linear regression of the experimental data. As this figure shows, the effect of silver addition is complete at silver contents as low as 3%.

DISCUSSION

During the room temperature CO-deposition process onto the Ru/SiO_2 catalyst, formation of CO_2 was not detected. If, under the conditions of the adsorption process

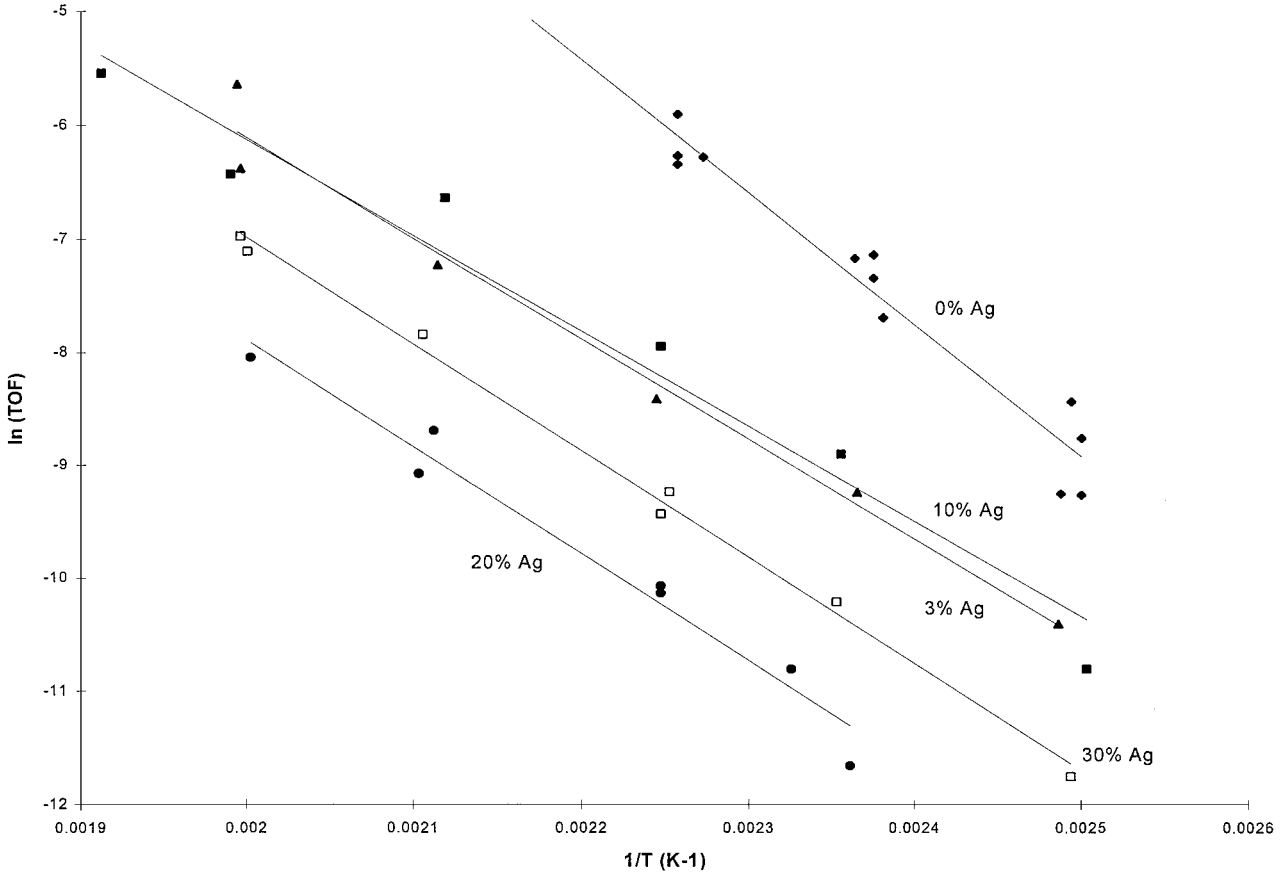

FIG. 7. Arrhenius plot for methane formation over Ag–Ru/SiO_2.

(1 atm, 298 K), atomic carbon is deposited via the Boudouard reaction, then one would expect to detect CO_2 formation upon exposure to CO. Conversely, if the CO adsorbs molecularly on the catalyst surface, then no CO_2 would be expected to form. In addition, the formation of water upon exposure of the catalyst to hydrogen requires the presence of adsorbed oxygen. For these reasons, it is assumed that the CO adsorbed on the catalyst in this study does so without loss of the oxygen. Early studies by Rabo *et al.* (58) also did not detect CO disproportionation to CO_2 during room temperature adsorption of CO over silica-supported Ru. This study also noted that no reaction took place upon exposure of this chemisorbed CO to hydrogen gas at room temperature. As mentioned previously, such low-temperature adsorption on ruthenium is believed to be molecular and not dissociative, resulting in a metal-to-CO ratio of 1 : 1. It is possible that dissociation of the molecularly adsorbed CO may occur upon heating of the catalyst surface to reaction temperatures prior to exposure to hydrogen. However, since this dissociation would require the formation of metal–oxygen bonds on a surface already saturated with chemisorbed CO, dissociation would require desorption of CO as metal–carbon bonds are broken in favor of metal–oxygen bonds. As desorption of CO during heating was not observed, it is assumed that the metal-to-carbon ratio remained at unity. This is in agreement with the studies of Duncan and Root (59) and Mizushima *et al.* (60), who reported that CO desorption from supported Ru catalysts does not occur until about 573 K.

Deactivation of the Ru surface through irreversible atomic carbon deposition was not found to occur to a detectable degree under the conditions of these experiments, as is evident from the relatively constant calibration factor values obtained for each experiment (57). The calibration factors are equal to the integrated area under the total methane (mass spectrometer) signal for each experiment as the reaction is driven to completion, and this area is directly proportional to the total amount of methane formed. Had appreciable deactivation been occurring through the course of the experiments, less and less methane would be formed with each successive experiment, and one would expect to see a change in the calibration factors to lower values.

The TOF values obtained in this study are similar to those obtained by others in steady-state experiments (11, 18, 61–63), as shown in Table 2, where the maximum TOF for this

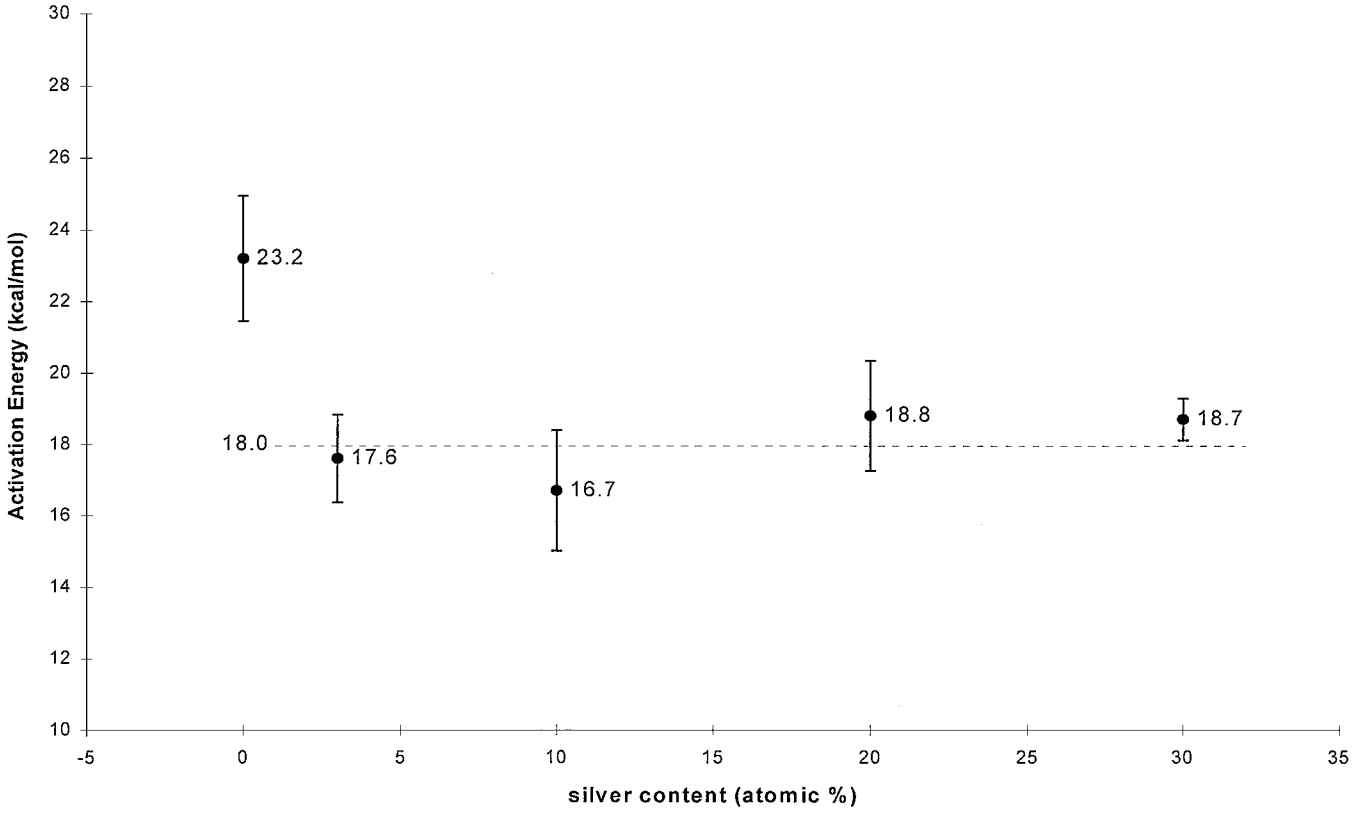

FIG. 8. Effect of silver addition on apparent activation energy.

study is listed for comparison with the higher temperatures of other studies. The deviation from linearity in the TOF at high temperatures is likely due to diffusion effects interfering with the spectrometer response at these temperatures, which limit the maximum measurable TOF in this system to around 0.01 s^{-1}. Fortunately, these are the highest rates monitored during the course of this study, since the addition of other metals to Ru results in significantly lower TOF values. The value of the activation energy, 23.2 kcal mol^{-1}, is also in good agreement with the steady-state results of others. Since the rate-determining step in the mechanism of CO hydrogenation is the hydrogenation of surface carbon species, the adsorption of CO does not affect kinetic results. Therefore, comparison of results from steady-state studies and experiments that utilize preadsorbed CO is justified.

Our earlier NMR studies have identified three resonances representating hydrogen adsorbed on ruthenium (31). They have been labeled and described as α_I, strongly bound, low-pressure hydrogen; α_M, weakly bound, low-pressure hydrogen; and β, weakly bound, high-pressure

TABLE 2

Comparison of Kinetic Parameters for Methanation over Supported Ru

Author	Support	Temp. (K)	Pressure (atm)	E_a (kcal/mol)	CH_4 TOF[a] (/s)
Della Betta *et al.* (60)	Al_2O_3	473–610	0.75	24	0.020[b]
Vannice (11)	Al_2O_3	478–503	1.0	24.2 ± 1.2	0.181[b]
Ekerdt and Bell (61)	SiO_2	464–548	0.49	24.1	0.311[b,c]
Vannice (62)	SiO_2	478–503	1.0	27.0	0.068[b]
Bajusz and Goodwin (19)	SiO_2	510–540	0.75	19.5	0.062[d]
This study	SiO_2	400–500	0.61	23.2 ± 1.8	0.056

[a] 548 K (extrapolated if necessary).
[b] $H_2/CO = 3$.
[c] At steady state.
[d] $H_2/CO = 20$.

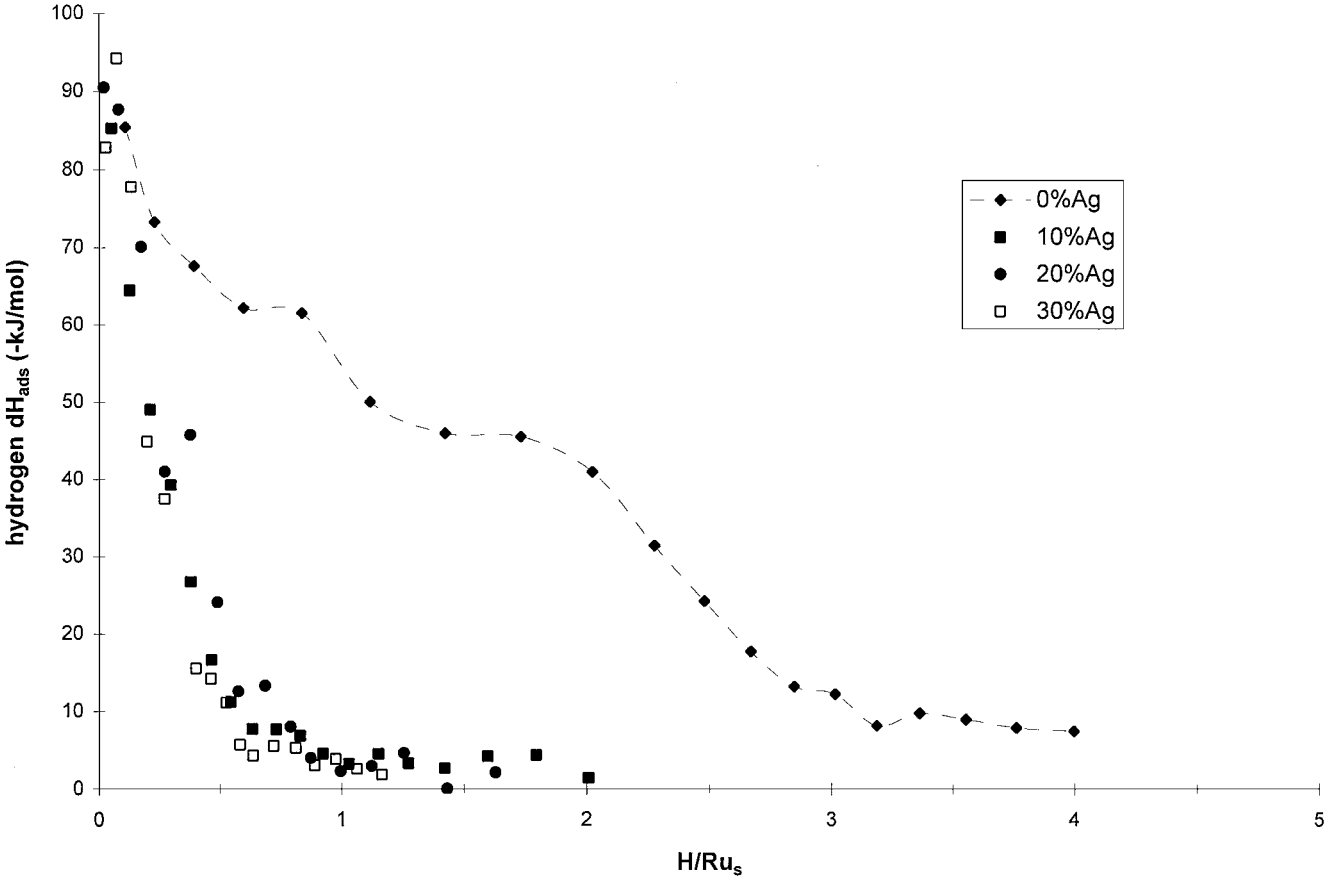

FIG. 9. Differential hydrogen adsorption enthalpy on Ag–Ru/SiO_2, 403 K (51).

hydrogen. The α_I resonance typically occurs at about -60 ppm, whereas the α_M and β resonance peaks have pressure-dependent shifts of about -55 and -45 ppm (± 10 ppm), respectively. The two resonance peaks found in Fig. 4 correspond to the weakly bound α_M and β hydrogen species. These two hydrogen species are known to exchange rapidly with the gas phase, and the β species is thought to be an absorptive precursor to the α species, and is thus partially associated with gas phase hydrogen (31). The asymptotic hydrogen coverage of 2.5 H/Ru$_s$ in Fig. 9 has been confirmed by previous studies on this catalyst (25) in the absence of adsorbed CO, and by earlier unpublished work. Direct comparison of these data with that from CO-free adsorption studies is justified since it has been shown that the surface carbon is nearly completely depleted after 30 min. For this reason, the higher coverage data in this figure represents hydrogen adsorption on a surface with very little CO present.

If experimental conditions are such that few unoccupied sites exist on the catalyst at any given time, and that any products formed rapidly desorb, then $\theta_{CO} \approx 1 - \theta_H$ and Eq. [1] simplifies to

$$\text{rate} = k\left(\theta_H - \theta_H^2\right). \qquad [2]$$

This equation is consistent with the data in Fig. 6, which shows a symmetric increase and decrease in the rate about a central coverage of hydrogen. The first and second derivatives of Eq. [2] show that the maximum rate should occur at $\theta_H = 0.5$. However, since θ represents relative coverages, its value is limited between 0 and 1, while H/Ru$_s$ is not limited, and varies from 0 to 2.5 under these conditions. If it is assumed that an H/Ru$_s$ coverage of 2.5 corresponds approximately to $\theta_H = 1$, then the rate should maximize at H/Ru$_s$ = 1.25, which is not far from the observed value of 1.1. Therefore, it appears that the kinetic derivations presented earlier are supported by these NMR results.

The background information previously presented on bimetallic Group IB–Ru catalysts stressed the dramatic effect that addition of the Group IB metal has on the catalytic behavior of transition metals, and this effect is well represented in Fig. 7. Our previous CO hydrogenation studies on silica-supported Group IB–Ru catalysts (49) also reported large decreases in activity for the Ag–Ru series, with the TOF for CO consumption decreasing rapidly up to a Ag content of 20%. At higher Ag loadings, only marginal changes were evident. Our Monte Carlo simulations of Ag–Ru catalysts indicate that this loading corresponds to nearly complete occupation of all low-coordination sites by Ag.

TABLE 3

Rate Decreases during CO Hydrogenation upon Addition of Ag to Ru Catalysts

Author	Support	Temp.	Pressure	Ag : Ru	TOF change
Enomoto (47)	Al_2O_3	493 K	0.66 atm	50 : 50	−76%[a]
Kelzenberg (48)	SiO_2	523 K	11.0 atm	13 : 87	−18%[a]
				30 : 70	−58%[a]
This study	SiO_2	473 K	0.61 atm	10 : 90	−76%[b]
				30 : 70	−93%[b]

[a] CO consumption.
[b] CH_4 formation.

Table 3 (48, 49) compares these results with those of previous similar studies. Although this table shows wide variations in the measured effect of Ag addition on reaction rates, the general trend of a strong reduction in the specific activity of Ru is the same in all cases, even at Ag loadings as low as 10%. To the authors' best knowledge, no activation energy measurements for CO hydrogenation have previously been made on Ag–Ru catalysts for comparison.

The observed decrease in apparent activation energy for CO hydrogenation upon addition of Ag to Ru/SiO_2 in Fig. 8 can be interpreted as follows. From the expression for the reaction rate given by Eq. [1], since all surface reactions are rapid and any products desorb rapidly, a site balance yields

$$\text{rate} = k\theta_{\text{H}}(1 - \theta_{\text{H}} - \theta_*). \qquad [3]$$

The portion of the experiment from which kinetic data is gathered, at maximum rate, occurs after initiation of the surface reaction, when hydrogen is rapidly adsorbing onto the surface and reacting with adsorbed CO which is still readily available. During this period, gas phase hydrogen is in near equilibrium with surface hydrogen, and the population of vacant surface sites is very small and approximately constant. The first assumption of hydrogen equilibrium leads to

$$\text{rate} = k[(K_{\text{H}}P_{\text{H}})^{1/2}\theta_* - K_{\text{H}}P_{\text{H}}\theta_{**}^2 - (K_{\text{H}}P_{\text{H}})^{1/2}\theta_*^2], \qquad [4]$$

and the second assumption, that $\theta_* \ll 1$, or $\theta_*^2 \ll \theta_*$, suggests

$$\text{rate} \approx k\theta_*(K_{\text{H}}P_{\text{H}})^{1/2}. \qquad [5]$$

This expressions shows that the reaction rate for this experiment is a function of the partial pressure of hydrogen gas and the equilibrium constant for adsorption on a particular surface.

In processes where the kinetics of adsorption may influence reaction rates, transition state theory (TST) can be used to show the relationship between observed, or apparent, activation energies and heats of adsoprtion of reactants. The use of transition state theory is necessary in order to relate properties of the transition state activated complex, such as the activation energy, with rate parameters for the overall process. According to TST, the rate constant k for a reaction can be expressed in terms of a pseudo equilibrium constant, K'', between the reacting species and the transition state activated complex (64):

$$k = \frac{k'T}{h}K''. \qquad [6]$$

The pseudo equilibrium constant is related to the usual thermodynamic state functions by

$$\Delta G^\circ = -RT\ln K'' = \Delta H^\circ - T\Delta S^\circ, \qquad [7]$$

where the thermodynamic variables represent the difference of the state functions between the activated complex and reactants referenced to a particular, common ground state. Equation [6] can now be expressed as

$$k = \frac{k'T}{h}\exp\left(\frac{\Delta S^\circ}{R}\right)\exp\left(-\frac{\Delta H^\circ}{RT}\right). \qquad [8]$$

Differentiation of the logarithm of this equation with respect to temperature (at constant pressure) defines the activation energy for the process under consideration and yields

$$\left(\frac{\partial \ln k}{\partial T}\right)_P \equiv \frac{E_{\text{a}}}{RT^2}, \qquad = \frac{\Delta H^\circ + RT}{RT^2}. \qquad [9]$$

Therefore, $E_{\text{a}} = \Delta H^\circ + RT$, and Eq. [8] is now

$$k = \left[\frac{ek'T}{h}\exp\left(\frac{\Delta S^\circ}{R}\right)\right]\exp\left(-\frac{E_{\text{a}}}{RT}\right). \qquad [10]$$

Readers are referred to Amdur and Hammes (64), Moulijn (65), and Boudart (66) for more lengthy discussions and detailed derivations.

The equilibrium constants for adsorption are given by

$$\ln K^{1/2} = -\frac{\Delta G_{\text{ads}}}{2RT}. \qquad [11]$$

Substitution of Eqs. [10] and [11] into Eq. [5] yields

$$\text{rate} = \left[\frac{ek'T}{h}\theta_* P_{\text{H}}^{1/2}\exp\left(\frac{\Delta S^\circ}{R}\right)\right]\exp\left(-\frac{\left(E_{\text{a}} + \frac{1}{2}\Delta G_{\text{ads}}^{\text{H}_2}\right)}{RT}\right). \qquad [12]$$

Substitution of the thermodynamic relation $\Delta G =$

$\Delta H - T\Delta S$ gives the final result:

$$\text{rate} = \left[\frac{ek'T}{h}\theta_* P_{\text{H}}^{1/2} \exp\left(\frac{\left(\Delta S^\circ + \frac{1}{2}\Delta S_{\text{ads}}^{\text{H}_2}\right)}{R}\right)\right] \times \exp\left(-\frac{\left(E_{\text{a}} + \frac{1}{2}\Delta H_{\text{ads}}^{\text{H}_2}\right)}{RT}\right). \quad [13]$$

This equation shows that the observed activation energy, $E_{\text{a,obs}}$, obtained experimentally from an Arrhenius relation of the form

$$\ln \text{rate} = -\frac{E_{\text{a,obs}}}{RT} + \ln c \quad [14]$$

is related to the heat of hydrogen adsorption by (65)

$$E_{\text{a,obs}} = E_{\text{a}} + \frac{1}{2}\Delta H_{\text{ads}}^{\text{H}_2}. \quad [15]$$

In effect, Eq. [14] shows that, in a system where the kinetics of a rapid surface reaction are being slowed due to decreased reactant adsorption rates (manifested in an increase in the adsorption enthalpy of the reactants), the observed activation energy will be less than that in the previous case (since adsorption is exothermic) (64, 65).

Since the variables in these equations are all dependent on hydrogen coverage, it is important to note that variables such as ΔH_{ads} are more accurately written as the differential values over a given range of coverages, dH_{ads}. However, for simplicity, the integral representation for the variables will continue to be used. Comparison of Eqs. [13] and [14] to yield Eq. [15] requires that the entropy terms are either approximately constant within the temperature range considered or at least that these terms are small enough in magnitude compared to the activation energy and enthalpy to be considered constant. The exponential temperature dependence of the enthalpy term will obviously be larger than that of the entropy term, which does not contain a temperature factor, apart from its own temperature dependence. The second requirement is generally true for such systems, and for hydrogen adsorption on the catalysts in this study, ΔH_{ads} ranges between -5 and -95 kJ mol^{-1}, while ΔS_{ads} ranges from -20 to -170 J mol^{-1} K^{-1} (51).

Microcalorimetry data gathered earlier on these catalysts, reroduced in Figs. 9 and 10 (51), show that the differential heat of adsorption for hydrogen on the Ru and Ag–Ru catalysts at 400 K decreases with increasing hydrogen coverage and Ag content. The ^{1}H-NMR results for

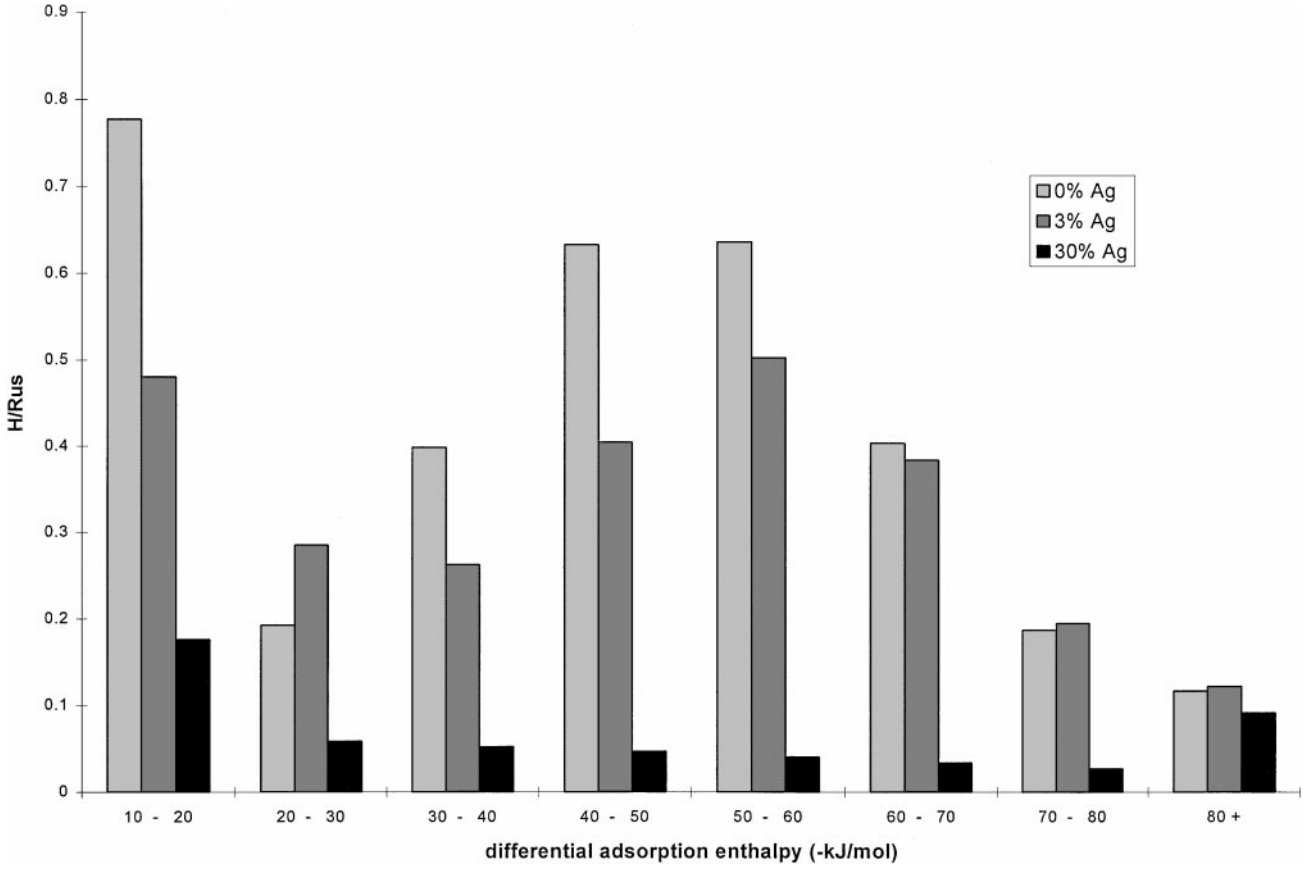

FIG. 10. Differential adsorption enthalpy distribution (51).

the monometallic catalyst presented earlier (Fig. 6) indicate that the coverage during the period of maximum rate at 400 K is between 1.0 and 1.1 H/Ru_s. From Fig. 9, this corresponds to a differential heat of adsorption of approximately -50 kJ mol^{-1}. Except for very low (initial) coverages, the adsorption enthalpy is higher at all coverages on the bimetallic catalysts. The presence of silver acts to increase the heat of adsorption of hydrogen, and Fig. 9 shows that adsorption enthalpies greater than -50 kJ mol^{-1} on the bimetallic catalysts correspond to hydrogen coverages between about 0.25 and 0.60 H/Ru_s before the enthalpy becomes negligible. Figure 10, derived from the data in Fig. 9, shows a distribution of adsorption states with similar adsorption enthalpies.

Clearly, the amount of hydrogen available on the surface for reaction is strongly reduced in the presence of silver, from about 1.1 H/Ru_s for Ru/SiO_2 to between 0.25 and 0.60 H/Ru_s in the Ag–Ru series. This corresponds to an increase in the differential heat of adsorption for hydrogen (at these coverages) from about -50 kJ mol^{-1} in the monometallic case to between -10 and -40 kJ mol^{-1} in the bimetallic series. Figure 10 shows the change in the distribution of adsorption states upon silver addition. As this figure shows, the states which were depopulated the most were those with adsorption enthalpies between -40 and -60 kJ/mol. This behavior is reflected in changes in the integral adsorption enthalpies for these catalysts, and the microcalorimetric studies in our laboratories (51) revealed a net increase in the integral heat of hydrogen adsorption upon addition of Ag to Ru/SiO_2. Indeed, using the activation energies calculated in this study, Eq. [15] shows that the difference in (integral) adsorption enthalpies for these two types of catalyst should be

$$\Delta H_{\text{ads}}^{H_2}\Big|_{\text{Ag–Ru}}^{\text{Ru}} \approx 2\left(E_{\text{a,obs}}^{\text{Ru}} - E_{\text{a,obs}}^{\text{Ag–Ru}}\right),$$
$$= 2\left(23.2\ \frac{\text{kcal}}{\text{mol}} - 18.0\ \frac{\text{kcal}}{\text{mol}}\right) = 43.5\ \frac{\text{kJ}}{\text{mol}}. \quad [16]$$

This value is within the range of the enthalpies of the most depopulated states in Fig. 10.

Analogous arguments can be made for similar bimetallic systems. For example, the effects of alkali promoters with ruthenium and other catalysts have been attributed to the restriction of surface hydrogen mobility by the alkali metal (67). The effects on reaction are not unlike those in the Ag–Ru system; in Ru systems, alkali metal atoms are known to occupy low-coordination sites and result in lower overall reaction rates, higher molecular weight product distributions, and increases in the product olefin-to-paraffin ratio. These observations can easily be attributed to restricted hydrogen adsorption on the surface, leading to slower reaction rates, more unsaturated CH_x species which incorporate into hydrocarbon chains, and fewer saturated terminating species. Marcelin *et al.* (35) examined the effect of alkali promotion of supported rhodium catalysts on hydrogen adsorption using frequency response chemisorption. The authors noted that such promotion resulted in almost complete loss of certain "kinetically distinct" adsorption sites.

Another example is the Cu–Ru system. While previous measurements of activation energies during CO hydrogenation have not been conducted on Ag–Ru catalysts, the results of this study clearly indicate an apparent decrease in the observed activation energy at all levels of Ag loading. However, previous studies of Cu–Ru systems have reported either no change in activation energy (68) or slight increases (49). In both systems, large decreases in specific Ru activity have been reported. The apparent disparity in measured activation energies between these two systems may be accounted for by differences in hydrogen adsorption characteristics of these systems. While neither Ag or Cu adsorbs hydrogen appreciably, spillover of hydrogen from Ru is known to occur for Cu (69), but not for Ag (47). Although the exact effects of this difference have not yet been completely elucidated, the ^{1}H-NMR study of Wu *et al.* (47) showed that Cu interacts with Ru more strongly that Ag, with less Cu than Ag being required to cover the same fraction of surface Ru. Chen and Goodwin's (70) description of Cu as acting as a "holding area" for hydrogen spillover to accommodate CO hydrogenation to CH_x species supports the observation of increased CH_4 selectivity by Cu during CO hydrogenation (68).

PORTAL SITE MEDIATED HYDROGEN ADSORPTION

The observed decrease in the specific activity of Ru in Ag–Ru systems in this study may be explained in terms of a phenomenon which we have referred to as "portal site mediated adsorption" (51, 57, 71). Figure 11 is a schematic of the operative surface processes in this model. According to this model, hydrogen adsorption occurs via two pathways. The first involves rapid, dissociative adsorption at low-coordination sites to produce weakly bound, highly mobile hydrogen. Similar adsorption and dissociation behavior has been shown to be more efficient at low-coordination sites on platinum (34). The second pathway is adsorption directly onto the basal planes, which occurs at an intrinsically slower rate (48). Since the weakly bound hydrogen adsorbed at low-coordination sites is highly mobile, it can then either migrate to strongly bound states, spill over to the support, or recombine with another hydrogen atom and desorb.

In the presence of adsorbed CO, the portal sites serve as "sinks" for gaseous hydrogen, supplying weakly bound, mobile surface hydrogen for reaction. When Ag occupies portal sites, it effectively closes the portals to hydrogen adsorption. Hydrogen must then adsorb directly onto the basal planes, a process which, as mentioned, occurs more slowly. Recombination and desorption of hydrogen, which is not affected to a large extent by the occupation of

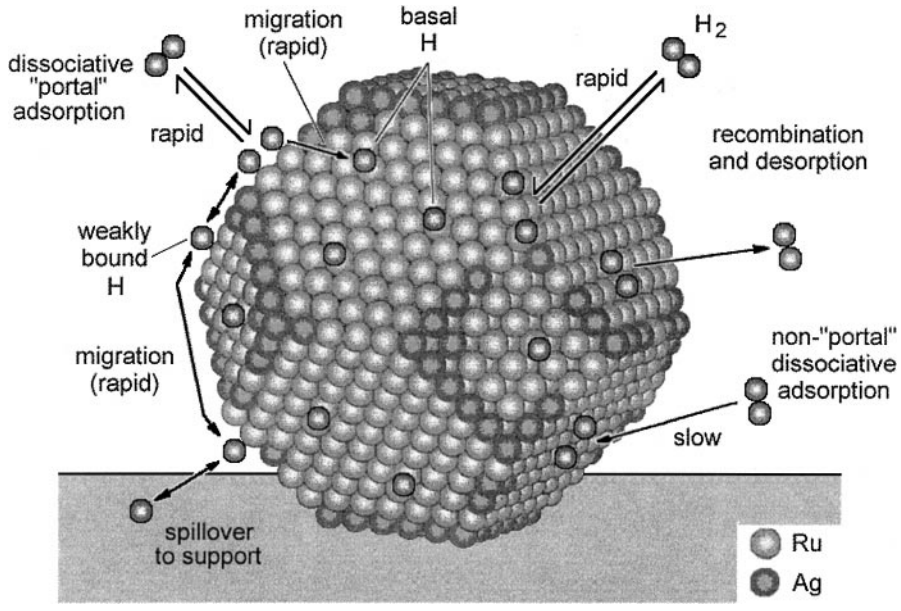

FIG. 11. Portal site mediated adsorption of hydrogen.

low-coordination sites by Ag, continues simultaneously. The net effect is a slowing of methane production due to decreased availability of surface hydrogen, which in effect alters the limiting kinetics of the overall process from surface reaction to adsorption of hydrogen.

This model is supported by previous microcalorimetric studies by our group (51) on the adsorption of hydrogen onto silica-supported Ru and Ag–Ru catalysts. In these studies, we noted the following effects on addition of Ag to Ru catalysts: there was no significant change in the initial heat of hydrogen adsorption, between 90 and 95 kJ mol^{-1} (Fig. 9); the total amount of hydrogen adsorbed per ruthenium surface atom was significantly reduced; the reduction in adsorbed hydrogen was coupled with a loss in weak and intermediate hydrogen adsorption states, between 40 and 60 kJ mol^{-1} (Fig. 10); there was no significant change in the amount of strongly adsorbed hydrogen states above 80 kJ mol^{-1}. The fact that the initial heat of adsorption for these both types of catalysts are essentially the same suggests the absence of electronic ("ligand"), ensemble, or segregation effects which directly affect the chemisorptive bond or adsorption site. This is in agreement with previous ^{1}H-NMR studies, which showed no evidence for electronic (26) or ensemble (49, 52, 54) effects in Ag–Ru systems. This suggests that either low-coordination sites do not have significantly different heats of adsorption or that there are too few of these sites to resolve them in microcalorimetry (51).

Since it is known that Ag atoms preferentially occupy low-coordination edge and corner sites in Ag–Ru/SiO_2 catalysts, the observed loss of low-to-intermediate adsorption states is coupled with the loss of low-coordination sites for hydrogen adsorption on these surfaces. Several possibilities exist to explain this observation: electronic effects, blocking or other geometric site alterations, or changes in the kinetics of hydrogen adsorption. As previously discussed, electronic effects are not considered to be operative in this system. Although Ag blocks low-coordination sites, these sites would each have to accommodate 10–20 hydrogen atoms to account for the large losses of hydrogen observed (51). In addition, this second possibility is unlikely due to the previously mentioned high mobility of hydrogen under these conditions. The third alternative is accounted for by the portal site mediated adsorption model. Under this model, any weakly bound hydrogen that is able to adsorb either migrates to strongly bound states, spills over to the support, or recombines and desorbs. The simultaneous recombination and desorption of surface hydrogen takes place at relative rates, according to the adsorption states of the two atoms combining: weak–weak > weak–strong > strong–strong. Thus, the strongly bound hydrogen remains on the surface longer and accumulates. However, since the replentification of weakly bound surface hydrogen at portal sites is being blocked by Ag in the bimetallic system, the net effect is a depopulation of weakly bound states.

This view is supported by results of recent studies using ^{1}H-NMR, which showed the rates of hydrogen adsorption being dramatically lowered on bimetallic catalysts and decreases in measured hydrogen sticking coefficients on Ag–Ru (72). In addition, the fact that the microcalorimetry results clearly show an increase in the average heat of adsorption of hydrogen on these catalysts supports the observations of previous reaction studies. These studies (50, 54) showed a decrease in the order of reaction of hydrogen from

−1.5 to −2.5 upon addition of Ag to Ag–Ru/SiO_2 during ethane hydrogenolysis, an effect which is the same as if the heat of adsorption of hydrogen was greater on the bimetallic catalyst (51).

Besides partially explaining the differences in observations of Ag–Ru adsorption studies, the implications of this study may also help resolve the inconsistent results of reaction surface sensitivity studies by examining CO hydrogenation. While the catalytic hydrogenation of CO may indeed be structure insensitive, the fact that this study suggests that the adsorption of hydrogen is structure sensitive may explain the inconsistency of experimental results where hydrogen adsorption is assumed to be at equilibrium and occurring much more rapidly than the surface reaction. In fact, this study shows that, under certain circumstances, adsorption effects may affect the kinetics of surface reactions and thus are responsible for apparent surface reaction sensitivity.

APPENDIX: NOMENCLATURE

ΔG°	Gibbs free energy difference between transition state and ground state
ΔH°	enthalpy difference between transition state and ground state
ΔS°	entropy difference between transition state and ground state
ΔG_{ads}	Gibbs free energy of adsorption
ΔH_{ads}	enthalpy of adsorption
ΔS_{ads}	entropy of adsorption
θ	surface coverage
c	arbitrary constant
e	exponential constant, 2.7183
E_a	activation energy
$E_{a,obs}$	observed, or apparent, activation energy
h	Planck's constant, 6.624×10^{-14} J s
k	rate constant
k'	Boltzmann's constant, 1.3805×10^{-16} erg/(molecule K)
K''	pseudo equilibrium constant between ground and transition states
K	adsorption equilibrium constant
P	partial pressure
r	rate of reaction
R	universal gas constant, 8.314 J/(mol K)
T	absolute temperature, K

ACKNOWLEDGMENTS

The authors would like to thank the U.S. Department of Energy Ames Laboratory, Iowa State University, and the Department of Chemical Engineering for providing the necessary resources to complete this work. Funding for this project was provided by the U.S. Department of Energy, Office of Basic Energy Sciences, Division of Chemical Sciences under Contract W-7405-ENG-82 and by the National Science Foundation through Engineering Research Equipment Grant CBT-8507418. Special thanks to Dr. Naresh Kumar, Dr. R. Lakshmi Narayan, and Dr. Nilesh Savargaonkar for sharing their previous work in this area and Eric Lee of Ames Laboratory for his assistance with the NMR instrumentation.

REFERENCES

1. Sabatier, P., and Senderens, J. B., *C. R. Hebd. Seances Acad. Sci.* 514 (1902).
2. Fischer, F., and Tropsch, H., *Brennst.-Chem.* **4**, 276 (1923).
3. Biloen, P., and Sachtler, W. M. H., *Adv. Catal.* **30**, 165 (1981).
4. Wender, I., *Fuel Process. Technol.* **48**, 189 (1996).
5. Dry, M. E., *Appl. Catal. A* **138**, 319 (1996).
6. Fan, L., Yan, S., Fujimoto, K., and Yoshii, K., *J. Chem. Eng. Jpn.* **30**(5), 923 (1997).
7. Fiato, R. A., *Top. Catal.* **2**(1–4), (1995).
8. Adesina, A. A., *Appl. Catal. A* **138**, 345 (1996).
9. Bartholomew, C. H., *in* "New Trends in CO Activation, Studies in Surface Science and Catalysis" (L. Guczi, Ed.), Vol. 64. Elsevier, Amsterdam, 1991.
10. Somorjai, G. A., *Catal. Rev. Sci. Eng.* **23**(2), 189 (1981).
11. Vannice, M. A., *J. Catal.* **37**, 462 (1975).
12. Fujita, S. I., and Takezawa, N., *Chem. Eng. J.* **68**, 63 (1997).
13. Hussain, S. T., and Atta, M. A., *Turk. J. Chem.* **21**, 77 (1997).
14. Zakumbayeva, G. D., Shapovalova, L. B., Yefremenko, I. G., and Gabdrakipov, A. V., *Petrol. Chem.* **36**(5), 428 (1996).
15. Haddad, G. J., and Goodwin, J. G., Jr., *J. Catal.* **157**, 25 (1995).
16. Janardaranao, M., *Ind. Eng. Chem. Res.* **29**, 1735 (1990).
17. Alstrup, I., *J. Catal.* **151**, 216 (1995).
18. Goodman, D. W., Kelley, R. D., Madey, T. E., and Yates, J. T., *J. Catal.* **63**, 226 (1980).
19. Bajusz, I. G., and Goodwin, J. G., Jr., *J. Catal.* **169**, 157 (1997).
20. Biloen, P., Helle, J. N., and Sachtler, W. M. H., *J. Catal.* **58**, 95 (1979).
21. Rabo, J. A., Risch, A. P., and Poutsma, M. L., *J. Catal.* **53**, 295 (1978).
22. Wentreck, P. R., Wood, B. J., and Wise, H., *J. Catal.* **43**, 363 (1976).
23. Gupta, N. M., Londe, V. P., and Kamble, V. S., *J. Catal.* **169**, 423 (1997).
24. Christmann, K., *in* "Surface Science Reports," Vol. 9, No. 1–3, p. 24. North-Holland Publishing, Amsterdam, 1988.
25. Bhatia, S., Engelke, F., Pruski, M., Gerstein, B. C., and King, T. S., *J. Catal.* **147**, 455 (1994).
26. Narayan, R. L., Savargaonkar, N., Pruski, M., and King, T. S., *in* "Studies in Surface Science and Catalysis" (J. W. Hightower, W. N. Delgass, E. Iglesia, and T. Bell, Eds.), Vol. 101, p. 921. Elsevier, Amsterdam, 1996.
27. Uner, D. O., Pruski, M., and King, T. S., *J. Catal.* **156**, 60 (1995).
28. Wu, X., Gerstein, B. C., and King, T. S., *J. Catal.* **135**, 68 (1992).
29. Pliskin, W. A., and Eischens, R. P., *Z. Phys. Chem.* **24**, 11 (1964).
30. Wu, X., Gerstein, B. C., and King, T. S., *J. Catal.* **118**, 238 (1989).
31. Engelke, F., Bhatia, S., King, T. S., and Pruski, M., *Phys. Rev. B* **49**, 2730 (1994).
32. Londe, V. P., and Gupta, N. M., *J. Catal.* **169**, 415 (1997).
33. Londe, V. P., Kamble, V. S., and Gupta, N. M., *J. Mol. Catal. A* **121**, 33 (1997).
34. Bernasek, S. L., and Somerjai, G. A., *J. Chem. Phys.* **62**(8), 3149 (1975).
35. Marcelin, G., Lester, J. E., and Goodwin, J. G., Jr., *Am. Chem. Soc. Prepr.–Div. Pet. Chem.* **30**(1), 189 (1985).
36. Riberio, F. H., Schach von Wittenau, A. E., Bartholomew, C. H., and Somorjai, G. A., *Catal. Rev. Sci. Eng.* **39**(1–2), 49 (1997).
37. Underwood, R. P., and Bennett, C. O., *J. Catal.* **86**, 245 (1984).
38. Bartholomew, C. H., *in* "New Trends in CO Activation" (L. Guczi, Ed.), Vol. 64, p. 158. Elsevier, Amsterdam, 1991.
39. Kelley, R. D., and Goodman, D. W., *Surf. Sci.* **123**, L743 (1982).
40. Iglesia, E., Soled, S. L., and Fiato, R. A., *J. Catal.* **137**, 212 (1992).
41. Johnson, B. G., Bartholomew, C. H., and Goodman, D. W., *J. Catal.* **128**, 231 (1991).

42. Somorjai, G. A., "Introduction to Surface Chemistry and Catalysis," p. 491. John Wiley & Sons, New York, 1994.
43. Wu, X., Gerstein, B. C., and King, T. S., *J. Catal.* **121**, 271 (1990).
44. Christmann, K., and Ertl, G., *J. Mol. Catal.* **25**, 31 (1984).
45. Goodman, D. W., and Peden, C. H. F., *Ind. Eng. Chem. Fundam.* **25**, 58 (1986).
46. Sinfelt, J. H., "Bimetallic Catalysts." Wiley, New York, 1983.
47. Wu, X., Gerstein, B. C., and King, T. S., *J. Catal.* **123**, 43 (1990).
48. Enomoto, T., Okuhara, T., and Misono, M., *Bull. Chem. Soc. Jpn.* **58**, 1490 (1985).
49. Kelzenberg, J. C., and King, T. S., *J. Catal.* **126**, 421 (1990).
50. Smale, M. W., and King, T. S., *J. Catal.* **119**, 441 (1989).
51. Narayan, R. L., and King, T. S., *Thermochim. Acta* **312**(1–2), 105 (1998).
52. Strohl, J. K., and King, T. S., *J. Catal.* **116**, 540 (1989).
53. Chuang, S. S. C., and Pien, S. I., *J. Catal.* **138**, 536 (1992).
54. Smale, M. W., and King, T. S., *J. Catal.* **120**, 335 (1990).
55. Sakakini, B. H., *J. Mol. Catal. A* **127**, 203 (1997).
56. Engelke, F., Vincent, R., King, T. S., and Pruski, M., *J. Chem. Phys.* **101**(9), 7262 (1994).
57. VanderWiel, D. P., Ph.D. Dissertation, Iowa State University, Ames, Iowa, 1998.
58. Rabo, J. A., Risch, A. P., and Poutsma, M. L., *J. Catal.* **53**, 295 (1978).
59. Duncan, T. M., and Root, T. W., *J. Phys. Chem.* **92**, 4426 (1988).
60. Mizushima, T., Tohji, K., and Udagawa, Y., *J. Phys. Chem.* **94**, 4980 (1990).
61. Dalla Betta, R. A., Piken, A. G., and Shelef, M., *J. Catal.* **35**, 54 (1974).
62. Ekerdt, J. G., and Bell, A. T., *J. Catal.* **58**, 170 (1979).
63. Vannice, M. A., *J. Catal.* **50**, 228 (1977).
64. Amdur, I., and Hammes, G. G., "Chemical Kinetics." McGraw-Hill, New York, 1966.
65. Moulijn, J. A., van Leeuwen, P. W. N. M., and van Santen, R. A., Eds. *in* "Studies in Surface Science and Catalysis," Vol. 79. Elsevier, Amsterdam, 1993.
66. Boudart, M., "Kinetics of Chemical Processes." Butterworth-Heinemann, Boston, 1991.
67. Uner, D. O., *Ind. Eng. Chem. Res.* **37**, 2239 (1998).
68. Luyten, L. J., van Eck, M., van Grondelle, J., and van Hooff, J. H., *J. Phys. Chem.* **82**, 2000 (1978).
69. Chen, B., and Goodwin, J. G., Jr., *J. Catal.* **148**, 409 (1994).
70. Chen, B., and Goodwin, J. G., Jr., *J. Catal.* **158**, 511 (1996).
71. Kumar, N., Vigil, R. D., and King, T. S., submitted for publication.
72. Savargaonkar, N., Narayan, R. L., Pruski, M., Uner, D. O., and King, T. S., *J. Catal.* **178**, 26 (1998).